Dual regulation of Stat1 and Stat3 by the tumor suppressor protein PML contributes to interferon α-mediated inhibition of angiogenesis

Kuo-Sheng Hsu[‡], Xuan Zhao[‡], Xiwen Cheng[‡], Dongyin Guan[‡], Ganapati H. Mahabeleshwar[§1], Yu Liu[‡], Ernest Borden[¶], Mukesh K. Jain[§], and Hung-Ying Kao[‡||2]

From the [‡]Department of Biochemistry and [§]Case Cardiovascular Research Institute, Case Western Reserve University, Cleveland, Ohio 44106, [¶]Taussig Cancer Institute, Cleveland Clinic Case Comprehensive Cancer Center, Cleveland Clinic Lerner College of Medicine of CWRU, Cleveland, Ohio 44195, and [||]The Comprehensive Cancer Center of Case Western Reserve University and University Hospitals of Cleveland, Cleveland, Ohio 44106

Edited by Xiao-Fan Wang

IFNs are effective in inhibiting angiogenesis in preclinical models and in treating several angioproliferative disorders. However, the detailed mechanisms of IFNα-mediated anti-angiogenesis are not completely understood. Stat1/2/3 and PML are IFNα downstream effectors and are pivotal regulators of angiogenesis. Here, we investigated PML's role in the regulation of Stat1/2/3 activity. In *Pml* knock-out (KO) mice, ablation of *Pml* largely reduces IFNα angiostatic ability in Matrigel plug assays. This suggested an essential role for PML in IFNα's anti-angiogenic function. We also demonstrated that PML shared a large cohort of regulatory genes with Stat1 and Stat3, indicating an important role of PML in regulating Stat1 and Stat3 activity. Using molecular tools and primary endothelial cells, we demonstrated that PML positively regulates Stat1 and Stat2 isgylation, a ubiquitination-like protein modification. Accordingly, manipulation of the isgylation system by knocking down *USP18* altered IFNα-PML axis-mediated inhibition of endothelial cell migration and network formation. Furthermore, PML promotes turnover of nuclear Stat3, and knockdown of *PML* mitigates the effect of LLL12, a selective Stat3 inhibitor, on IFNα-mediated anti-angiogenic activity. Taken together, we elucidated an unappreciated mechanism in which PML, an IFNα-inducible effector, possess potent angiostatic activity, doing so in part by forming a positive feedforward loop with Stat1/2 and a negative feedback loop with Stat3. The interplay between PML, Stat1/Stat2, and Stat3 contributes to IFNα-mediated inhibition of angiogenesis, and disruption of this network results in aberrant IFNα signaling and altered angiostatic activity.

Interferon α (IFNα) is a pleiotropic cytokine and an angiostatic factor that has been used to treat patients with angioproliferative diseases since the 1990s (1, 2). Although the anti-angiogenic effects of IFNα have been validated in *in vitro* and *in vivo* models, the detailed mechanisms remain unclear (3–9). In addition to angiostatic activity, IFNα signaling also plays important roles in stress responses, including inflammatory stresses, anti-viral infection, and anti-tumorigenesis. Upon binding to its membrane-bound receptors, IFN receptor 1 and 2, IFNα activates cytoplasmic tyrosine kinases, tyrosine kinase 2 and Janus tyrosine kinase 1 (JAK1) (2, 10, 11). This leads to subsequent phosphorylation of Stat1 at Tyr-701 (Tyr(P)-701-Stat1), which associates with Stat2, and interferon regulatory factor 9 (IRF9)[3] in a ternary complex, called the IFN-stimulated gene factor 3 (ISGF3). This is followed by nuclear translocation of ISGF3 and binding to specific DNA sequences in the promoters of a subset of IFN-stimulated genes to regulate their transcription, several of which are angiostatic (12, 13). In parallel with Stat1 activation, IFNα also induces transient phosphorylation of Tyr-705 of Stat3 (Tyr(P)-705-Stat3) and nuclear translocation in endothelial cells (ECs) (14). Interestingly, Stat1 and Stat3 antagonize each other's angiostatic and angiogenic activity, respectively (15, 16). Thus, it has been proposed that the balance between Stat1 and Stat3 activity, [Stat1]/[Stat3], determines the overall biological and pharmacological activity of IFNα (17, 18).

In addition to phosphorylation-dependent Stat1 and Stat3 activation, several post-translational modifications are also involved in IFNα signaling (11, 19, 20). For example, Stat1 is subjected to acetylation and Sumo1 and Isg15 (interferon-stimulated gene 15) conjugation (19, 21, 22). Of these modifications, acetylation and sumoylation negatively regulate Stat1 activity,

---

whereas the function of Isg15-linked Stat1 isgylation is poorly understood. Isg15 is highly induced by type I interferons, including IFNα and IFNβ. Protein isgylation, catalyzed by Isg15-activating E1 enzyme (Ube1L), Isg15-conjugating E2 enzyme (UbcH8), and Isg15 E3 ligase (HerC5), is a ubiquitination-like posttranslational modification that covalently conjugates Isg15 peptides to lysine residues of target proteins (20, 23). Isg15 conjugation is cleaved by the sole Isg15 deconjugating enzyme Usp18. The exact biological function of protein isgylation remains unclear but is known to play a role in the antiviral response and the control of protein stability (24, 25). Although it has been proposed that isgylation positively regulates JAK-Stat signaling and promotes Stat1-associated gene expression (26, 27), how Stat1 isgylation is regulated remains elusive. Furthermore, it is unclear whether other Stat family members involved in IFNα signaling such as Stat2 and Stat3 are also subjected to Isg15 conjugation.

The *PML* gene was originally isolated as a fusion partner of the human retinoic acid receptor α (RARα) in patients with acute promyelocytic leukemia (28–30). A significant fraction of PML is localized in discrete nuclear structures alternatively called Kremer bodies, nuclear domain 10, PML oncogenic domains, or PML nuclear bodies (NBs). Ablation of PML results in the loss of these structures and thereby changes PML-related biological functions, including transcriptional regulation, protein modification, apoptosis, and cellular senescence (31). *PML* is highly expressed in endothelium, and its mRNA levels are further elevated upon IFNα stimulation (6, 32). We recently showed that PML is essential for TNFα- and IFNα-mediated inhibition of EC migration and angiogenesis (6, 33). Furthermore, miR-1246 released from colon cancer cell-derived microvesicles, targets the *PML* mRNA 3′-UTR and down-regulates PML expression in HUVECs, thus promoting EC migration and tube formation (34). These results suggest that PML plays an important role in control of angiogenesis.

In this study we observed increased angiogenesis in *Pml* KO mice when treated with IFNα. This result suggested a pivotal role of PML in IFNα-mediated anti-angiogenesis. To further investigate the details, we found that PML has a dual function in this process. Upon IFNα stimulation, PML promotes ISGF3 activity for target gene expression and enhances Stat1/Stat2-mediated angiostatic effects in part through Stat1/Stat2 isgylation. Additionally, PML negatively regulates nuclear Stat3 stability and thus attenuates Stat3-mediated pro-angiogenic effects. Based on these findings, we propose a model in which PML plays an important role in IFNα-mediated Stat1/2 and Stat3 activation and disruption of PML blocked IFNα angiostatic ability.

Results

PML is required for IFNα-mediated angiostatic activity in vivo

We previously demonstrated that PML is essential for the ability of TNFα and IFNα to inhibit EC migration and capillary tube formation (6, 33). To further validate our *in vitro* data, we carried out *in vivo* Matrigel plug assays. *Pml* KO mice exhibited increased angiogenesis in the plugs compared with the wild-type mice (Fig. 1). Consistent with our previous *in vitro* data,
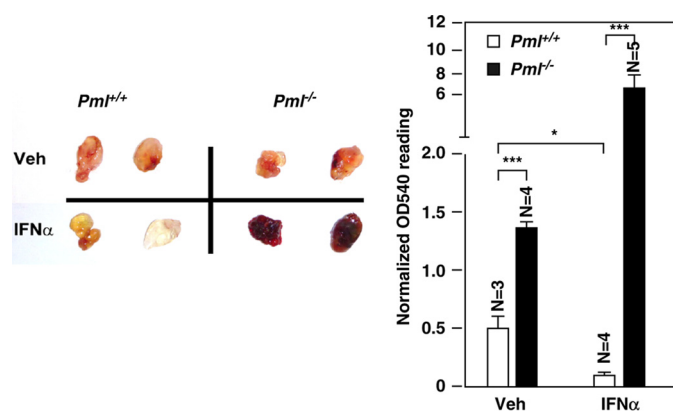

Figure 1. PML is required for IFNα-mediated angiostatic activity *in vivo*. *Left*, two representative Matrigel plugs from each group are shown. *Right*, quantification of angiogenesis. Approximately 200-mg plugs isolated from mice were homogenized in Drabkin's solution, and optical density was measured at 540 nm and normalized to the weight of the plugs. Unpaired two-tail *t* test (*, $p < 0.05$; ***, $p < 0.001$). The numbers (*N*) of mice are indicated for each group.

IFNα inhibited angiogenesis in the wild-type animals. However, significant increases in angiogenesis were observed in IFNα-treated *Pml* KO mice, suggesting that the ability of IFNα to inhibit angiogenesis is largely dependent on Pml. PML is also an IFNα-inducible gene. This observation indicates that PML is required for IFNα to inhibit angiogenesis *in vitro* and *in vivo*.

Depletion of PML promotes microvessel outgrowth and changes expression of IFNα- and Stat1-inducible genes

Because PML is highly expressed in human endothelium and our data also suggest PML as a key cytokine-inducible angiogenic inhibitor, we focused our study on endothelial system. To further dissect the role of PML in IFNα signaling, we examined PML and IFNα target genes. Earlier microarray data showed that knockdown (KD) of *PML* in HUVECs resulted in alterations of a set of target genes (35). Among these altered genes, IFNα-inducible genes (36) were significantly decreased in *PML* KD HUVECs (35). More than 100 genes that were induced >2-fold by IFNα in HUVECs were down-regulated >2-fold in *PML* KD cells. To validate this, we carried out quantitative real-time (qRT)-PCR and confirmed several IFNα and PML common target genes (Fig. 2*A*). These data suggest that loss of PML may compromise the ability of IFNα to induce its target genes. Stat1 is the major IFNα-induced transcription factor that is responsible for activation of numerous target genes. Cheon and Stark (37) reported that overexpression of a tyrosine phosphorylation-defective Stat1 mutant (unphosphorylated Stat1 (U-Stat1)) resulted in expression of several known interferon target genes, indicating that unphosphorylated Stat1 is transcriptionally active. Interestingly, these genes are down-regulated in *PML* knockdown cells as shown in our array (Fig. 2*B*). Stat1 and PML common target genes include *IFIT1*, *MX1*, *OAS1*, *OAS2*, *OAS3*, *IFI27*, *IFI44*, and *STAT1*. By qRT-PCR, we validated that these Stat1- and unphosphorylated Stat1-inducible genes are down-regulated in *PML* KD ECs (Fig. 2*C*). These data indicate that Stat1 induces *PML* expression in response to IFNα stimulation (6), and in turn, PML positively regulates Stat1 transcription activity.
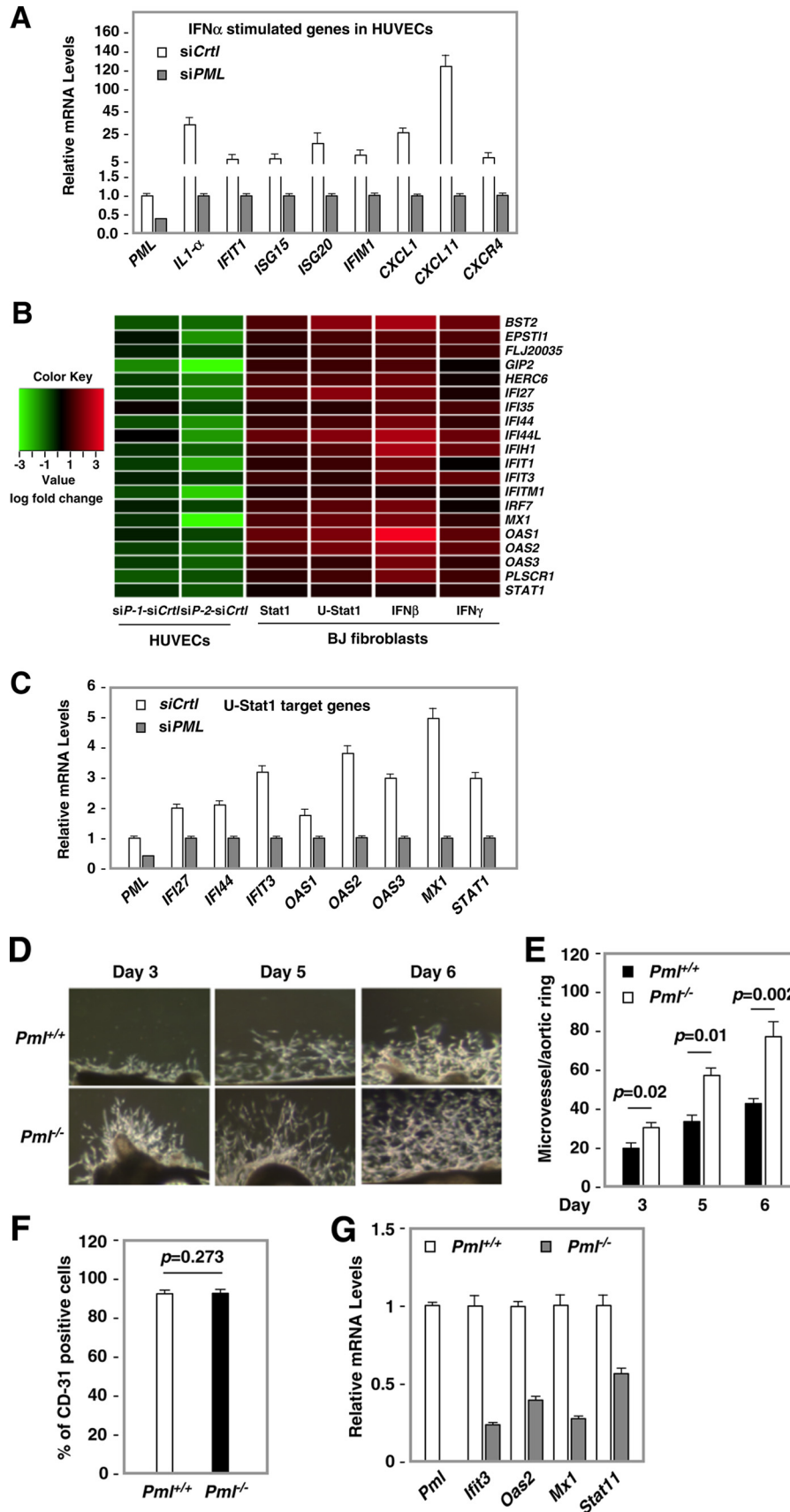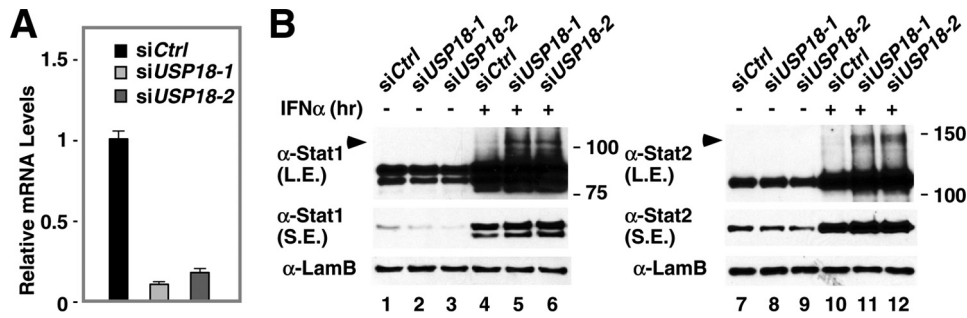
Figure 3. Long-term treatment of IFNα induced isgylation of Stat1 and Stat2. *A*, RT-qPCR of *USP18* mRNA accumulation. *B*, effect of *USP18* KD on Stat1 and Stat2 expression. HUVECs were transiently transfected with a control (si*Ctrl*) or two independent siRNAs (si*U-1* and si*U-2*) against *USP18*. 72 h after transfection cells were treated with vehicle or IFNα (10^3 units/ml) for 16 h. An aliquot of cells was used to isolate total RNA followed by RT-qPCR (*A*), and the rest of cells were used for subcellular fractionation (*B*). *L.E.*, long exposure; *S.E.*, short exposure.

To test whether the ability of Pml to regulate Stat1 target genes is conserved in mouse ECs, we isolated aortic rings from WT and *Pml* KO mice and carried out *ex vivo* aortic ring explant assays. We found that aortic rings isolated from *Pml* KO mice exhibited increased outgrowth of vessels compared with the rings from the wild-type animal (Fig. 2, *D* and *E*). Cells from aortic ring outgrowth were further isolated by FACS and confirmed as CD31-positive endothelial cells (38) (Fig. 2*F*). Isolated aortic ECs were grown and harvested, and total RNA was prepared. RT-qPCR demonstrated that the expression of Stat1 target genes such as *Ifit3*, *Oas2*, *Mx1*, and *Stat1* were significantly reduced in *Pml*−/− ECs (Fig. 2*G*).

PML promotes Stat1 and Stat2 isgylation and affects the ISGF3 complex

The transcriptional activity of Stat1 is regulated by IFNα-induced phosphorylation, nuclear translocation, acetylation, sumoylation, and Isg15 conjugation (isgylation). Although isgylation has been proposed to positively regulate Stat1 transcriptional activity, it is not clear whether this modification is present in ECs or how this modification is regulated (27, 39, 40). To address these issues, we determined the effect of IFNα and Usp18, the sole Isg15-deconjugating enzyme, on isgylation of nuclear Stat1 (nStat1). Due to the transient and reversible nature of this modification, the detectable levels of isgylated proteins are relatively low. To overcome this issue, HUVECs were transiently transfected with a control siRNA (si*Ctrl*) or two *USP18* siRNAs (si*USP18*) followed by IFNα treatment for 16 h and nuclear and cytoplasmic fractionation for Western blotting. RT-qPCR was performed to confirm that efficient knockdown of *USP18* was achieved (Fig. 3*A*). IFNα induced accumulation of nStat1 and a distinct slower migrating species (∼100 kDa) (Fig. 3*B*, *lanes 1 versus 4*). This Stat1 species was further induced in *USP18* KD cells (Fig. 3*B*, *lanes 5 and 6*, *L.E.*).

Similar observations were made for unmodified nuclear Stat2 and a slower migrating species of nStat2 (*lanes 7–12*, *arrowhead*). These results suggest that these slower-migrating proteins are likely to be Isg15-conjugated nStat1 (Isg15-nStat1) and nStat2 (Isg15-nStat2) and that knockdown of *USP18* significantly increased this modification. Similar to most post-translational modifications including acetylation, sumoylation, and methylation, only a small fraction of the Stat1 and Stat2 was isgylated.

To further verify whether these slower-migrating species are Isg15-conjugated Stat1 and Stat2, we performed immunoprecipitation followed by Western blotting. We first carried out knockdown experiments with a *control* (si*Ctrl*), *ISG15* (si*ISG15*), or *USP18* (si*USP18*) siRNA followed by a 16-h IFNα treatment. Knockdown of *ISG15* decreased protein isgylation, and knockdown of *USP18* increased the isgylation signal. Cells were harvested, and subcellular fractions were prepared. Nuclear fractions were immunoprecipitated with a control antibody, anti-Isg15, anti-Stat1, or anti-Stat2 antibody. Immunopellets were Western-blotted with anti-Stat1, anti-Stat2, or anti-Isg15 antibody. Our data indicate that endogenous Stat1 is isgylated in IFNα-treated HUVECs (Fig. 4, *A* and *B*) as well as Stat2 (Fig. 4, *C* and *D*). The observation of Stat1 isgylation is consistent with a previous report (21). Stat2 has not been previously reported to be Isg15-conjugated. Based on the mobility of the bands, we also detected unmodified Stat1 and Stat2 bands in the anti-Isg15 immunoprecipitates (Fig. 4, *B* and *D*, *lanes 7–9*, marked with *asterisks*). Together, these observations suggest that Stat1 and Stat2 are Isg15-conjugated.

We further carried out time-course experiments to determine whether isgylation of Stat1 and Stat2 occurs early or late after of IFNα stimulation. To investigate this, HUVECs were transiently transfected with a control or two independent

Figure 2. Depletion of *PML* promoted microvessel outgrowth and changed expression of IFNα and Stat1-inducible genes. *A*, qRT-PCR of IFNα-inducible genes in control and *PML* KD HUVECs. HUVECs were transiently transfected with a control siRNA or a mixture of two *PML* siRNAs. Total RNA was prepared 48 h post transfection followed by qRT-PCR using gene-specific primers. *B*, a heatmap representation of an array of genes that were significantly down-regulated in *PML* KD ECs (*lanes 1* and *2*) or significantly up-regulated in human fibroblasts (*BJ* cells) with overexpression of Stat1 (*lane 3*), U-Stat1 (*lane 4*), and treatment of IFNβ (*lane 5*) or IFNγ (*lane 6*) (data are from Cheon and Stark (37). The log-fold change was scaled in a *green-dark-red* color scheme. Each *row* represents a gene designated by the official gene symbol. Two independent *PML* siRNAs (*siP1* and *siP2*) was compared with a non-targeting control siRNA (*siC*). *C*, RT-qPCR of U-Stat1 target genes in *PML* KD ECs. HUVECs were transiently transfected with a non-targeting siRNA or a mixture of si*P-1* and si*P-2*. Total RNA was isolated 48 h after transfection followed by qRT-PCR. Relative mRNA levels are shown. *D*, representative pictures showing microvessel outgrowth in explanted aortic rings isolated from WT and *Pml*−/− mice at days 3, 5, and 6. Note that more microvessels sprouting from aortic rings prepared from *Pml*−/− mice than those isolated from the WT animals. *E*, quantification of microvessel outgrowth. *F*, cells from aortic ring outgrowth at the end of the experiments (12 days after explanting) were isolated and analyzed for CD31 expression by FACS analysis. *G*, aortic ECs were isolated from WT and *Pml*−/− mice as described in *F*. The expression of putative Stat1 target genes was quantified by RT-qPCR.
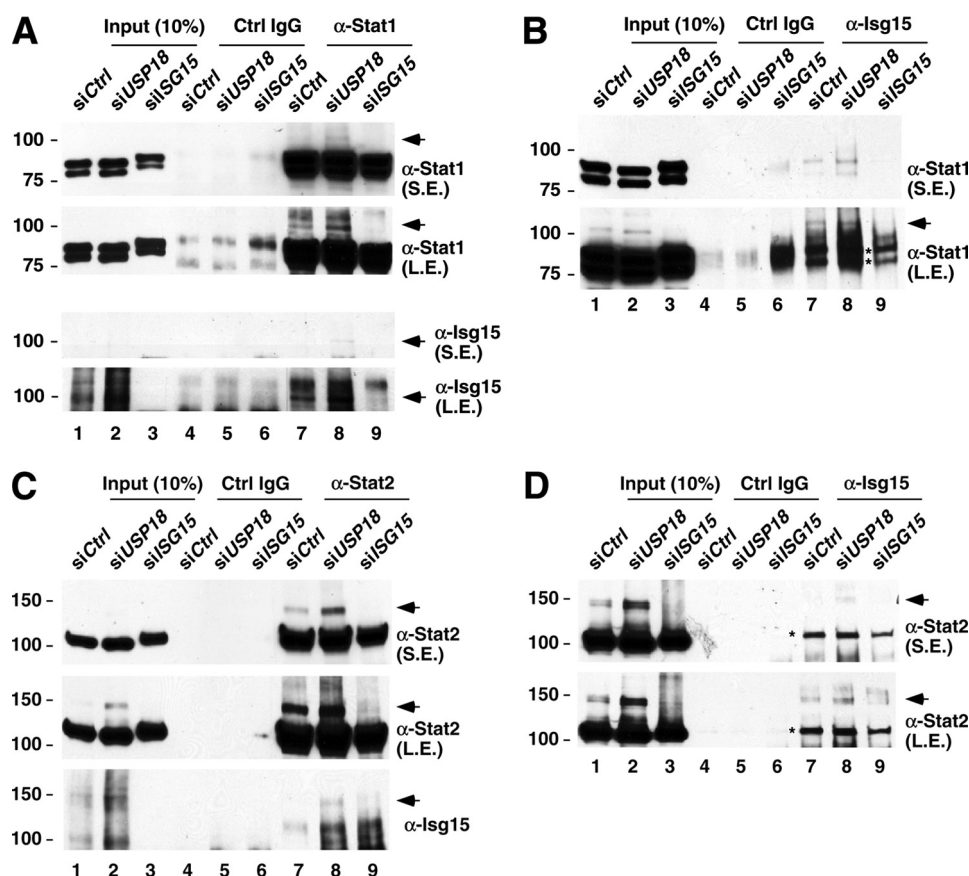
Figure 4. The effect of *USP18* or *ISG15* knockdown on Stat1 and Stat2 isgylation in response to IFNα treatment. HUVECs were transfected with a control, *ISG15*, or *USP18* siRNA. 72 h later cells were treated with vehicle or IFNα (10³ units/ml) for 16 h and harvested, and subcellular fractions were prepared. The nuclear fractions were used for immunoprecipitation with a control IgG, anti-Stat1 (*A*), Isg15 (*B* and *D*), or anti-Stat2 (*C*) antibodies. Ten percent of the input and the immunopellets were Western-blotted with anti-Stat1 (*A* and *B*), anti-Isg15 (*A* and *C*), or anti-Stat2 (*C* and *D*) antibodies. The *arrows* mark isgylated Stat1 or Stat2 (*A* and *C*). The *asterisks* mark unmodified Stat1 or Stat2 (*B* and *D*, *lane 7* and *8*). Because Isg15-Stat1 and Isg15-Stat2 are in low abundance, only a longer exposure of the film was able to detect these two species in the Input (10%) (*lanes 1–3*, data not shown). *S.E.*, shorter exposure; *L.E.*, longer exposure.

USP18 siRNAs, treated with IFNα, harvested at different time points, and analyzed by Western blotting. In the *siCtrl*-transfected ECs, we did not observe any difference in total protein levels of Stat1 or Stat2 for the first hour, but a significant increase in the levels of nStat1 and nStat2 was observed after 16 h of IFNα treatment (Fig. 5, *A* and *B*, *lanes 4 versus 8* and *lanes 12 versus 16*). Similar to that observed in Fig. 3*B*, a small fraction of a major slower-migrating Stat1 and Stat2 species was detected after a 16-h of IFNα treatment in control ECs (Fig. 5, *A* and *B*, *lanes 1– 4*). In *USP18* KD ECs, these slower migrating Stat1 and Stat2 species were increased (Fig. 5, *A* and *B*, *lanes 4 versus 8* and *lanes 12 versus 16*). However, we did not observe slower-migrating species of Stat3 in control or *USP18* KD HUVECs in response to IFNα stimulation, implying that Stat3 is not isgylated (Fig. 5*C*).

Previous studies that knockdown of *PML* decreased IFNα and Stat1 target gene expression suggest that knocking down *PML* might have an effect on posttranslational modification, nuclear translocation, or abundance of ISGF3 (Stat1, Stat2, and IRF9). To test this, HUVECs were transfected with a control siRNA or a *PML* siRNA, treated with IFNα, harvested, and nuclear and cytoplasmic fractions were prepared. Western blotting was performed with anti-Stat1, -Stat2, -Tyr-701-Stat1, and anti-IRF9 antibodies. In the control cells, in response to

IFNα treatment, we observed the following. 1) An additional nStat1 species appeared transiently at 0.5 h of IFNα (Fig. 6*A*, *lane 2*). This species is likely to be Tyr(P)-701-nStat1 (see Fig. 6*B*). 2) A significant increase appeared in nuclear Stat2, but not Stat1, at 0.5 h of IFNα treatment (Fig. 6*A*, *lanes 1 versus 2*). 3) A significant increase appeared in nStat1 and Stat2 at 16 h of IFNα treatment (Fig. 6*A*, *lane 5*). 4) A significant increase appeared in nuclear PML, Isg15, and IRF9 at 16 h of treatment (Fig. 6*A*, *lane 5*). 5) Isg15-conjugated nStat1 and Stat2 appeared at 16 h of IFNα treatment (*arrows*) (Fig. 6*A*).

Furthermore, knockdown of *PML* resulted in a marked decrease in Isg15-conjugated nStat1 and nStat2 at 16 h of IFNα treatment but had little or no effect on unmodified nStat1 and nStat2 (Fig. 6*A*, *lanes 5 versus 10*). Additionally, knockdown of PML significantly increased Isg15-conjugated and unmodified cytoplasmic Stat2. However, knockdown of PML did not decrease Tyr(P)-701-Stat1 (Fig. 6*B*, *lanes 2 versus 7*). These observations suggest that PML promotes Stat1 and Stat2 activity at a late stage of IFNα signaling by increasing Isg15 conjugation of nStat1 and Stat2. We further examined whether Pml regulates Isg15 conjugation of nStat1 and Stat2 in rodent ECs and found that loss of *Pml* resulted in decreases in Isg15-conjugated nStat1 and nStat2 (Fig. 6*C*, *lanes 4 and 8*) and blocked IFNα-induced nIRF9 (*lanes 2 and 6*) in mouse ECs.
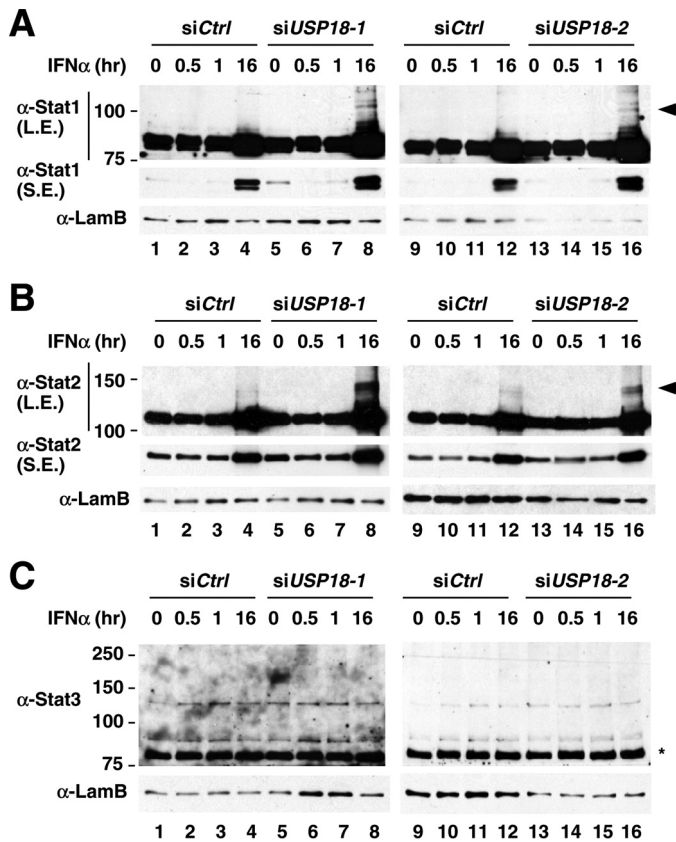
Figure 5. The effects of IFNα on Stat1, Stat2, and Stat3 protein. HUVECs were transiently transfected with a control siRNA (si*Ctrl*) or two independent *USP18* siRNA (si*U*). 48 h after transfection, equal numbers of cells were seeded, treated with IFNα, and harvested at indicated times. Subcellular fractions were prepared, and nuclear fractions were subjected to Western blotting with anti-Stat1 (*A*), anti-Stat2 (*B*), and anti-Stat3 (*C*) antibodies. The *arrows* mark the putative isgylated Stat1 (*A*) and Stat2 (*B*). The *asterisk* marks the unmodified Stat3 (*C*). *S.E.*, short exposure; *L.E.*, longer exposure.

The effect of USP18 knockdown on IFNα-mediated Stat1 isgylation, EC migration, and capillary tube formation

Our results indicated that loss of PML decreased nuclear isgylated Stat1 and Stat2 and nuclear IRF9 and reduced ISGF3 target gene expression. PML is angiostatic, as supported by both *in vitro* (6) and *in vivo* data (Figs. 1 and 2*D*). Our observations that knockdown of *USP18* increased isgylation of nStat1 and nStat2 (Figs. 3*B* and 5*A*, *lanes 4 versus 8* and *12 versus 16*) and that knockdown of *PML* decreased isgylation of nStat1 and nStat2 (Fig. 6*A*, *lane 5 versus 10*) suggested that USP18 is proangiogenic. To test this idea, we knocked down *USP18*, *PML*, or both in HUVECs and examined their effects on IFNα-mediated inhibition of EC migration and network formation. We found that knockdown of *USP18* increased Stat1 isgylation and decreased EC migration and capillary network formation (Fig. 7*A*, *lanes 1–3*, and Fig. 7*B*), whereas knockdown of *PML* did the opposite (Fig. 7, *B* and *C*). Furthermore, knockdown of *PML* compromised the *USP18* KD effects on Stat1 isgylation and EC migration and capillary tube formation (Fig. 7*A*, *lanes 4–6*, *B*, and *C*). Collectively, our data suggest that PML functions as an IFNα downstream effector to promote Stat1/2 isgylation and by this means enhances Stat1/2 transactivation of their gene expression and IFNα-mediated angiostatic activity.

PML negatively regulates nStat3 stability and attenuates Stat3 function in EC network formation

It has been proposed that Stat1 and Stat3 antagonize each other's activity (15, 16). Consistent with the notion, several Stat1-inducible genes described above (Fig. 2*C*) were repressed when Stat3 was overexpressed in A549 lung cancer cells (41). Using an siRNA KD approach and microarray hybridization, a recent study has examined gene expression patterns in control and Stat3 KD HUVECs (42) (data set no. GSM688389). We analyzed Stat3 target genes by perl and R programs and identified Stat3 target genes in HUVECs. Comparison of these Stat3 target genes with the PML target genes identified in our array study (35) suggested significant overlap. We found 426 genes that showed a >2-fold decrease in expression in *PML* KD ECs, 143 of which were induced >2-fold when *STAT3* was knocked down (supplemental Table 1). Furthermore, among 167 genes up-regulated >2-fold in *PML* KD ECs, 36 of which were found to be down-regulated >2-fold in *STAT3* KD ECs (supplemental Table 2). These observations indicate that PML and Stat3 share a large set of common target genes and that PML and Stat3 mutually antagonize a subset of each other's target genes.

To dissect the mechanism by which PML affects Stat3 expression in response to IFNα stimulation, we first examined whether knockdown of *PML* in HUVECs alters Tyr(P)-705-nStat3, nuclear translocation, or abundance of nStat3. In the control cells nStat3 and Tyr(P)-705-nStat3 significantly increased 0.5 h after IFNα treatment, markedly declined after 1 h of treatment, and Tyr(P)-705-nStat3 completely disappeared after 2 h of treatment (Fig. 8, *A* and *C*). These observations are consistent with previous reports indicating that Stat3 translocates to the nucleus in response to 0.5 h of IFNα treatment (14, 19). We further discovered that knockdown of *PML* 1) had little or no effect on nuclear translocation of Stat3 (Fig. 8*A*, *lanes 2* and *7*), 2) increased nStat3 accumulation after 1 h of IFNα treatment ~2-fold (Fig. 8, *A*, *lanes 8–10* and *B*), and 3) prolonged Tyr(P)-705-nStat3 (Fig. 8*C*, *lanes 2–4 versus 7–9*). These observations are significant because nStat3 antagonizes nStat1 activity, and a 2-fold increase in nStat3 accumulation will have a profound effect on IFNα signaling. In summary, these observations provide an important new finding that nStat3 abundance is altered by PML.

IFNα induces rapid nuclear translocation of Stat3. However, it remains unclear how nStat3 sharply declines afterward. Because the decrease in nStat3 occurs rapidly (0.5–1 h), we hypothesized that nStat3 is subjected to degradation after 0.5 h of IFNα treatment. To explore this possibility, HUVECs were treated with or without the proteasome inhibitor MG132 after 0.5 h of IFNα treatment. We found that MG132 increased nStat3 accumulation in IFNα-treated ECs, indicating that nStat3 is subjected to proteasome-mediated degradation after 0.5 h of IFNα stimulation (Fig. 8*D*). However, knockdown of *PML* blocked MG132-mediated increase in nStat3 accumulation (Fig. 8*E*).

Based on the transcriptome analysis from *PML* and *STAT3* KD HUVECs as well as biochemical data, we hypothesized that the increased Stat3 abundance observed in *PML* KD ECs contributes to elevated EC migration and angiogenesis. To test this
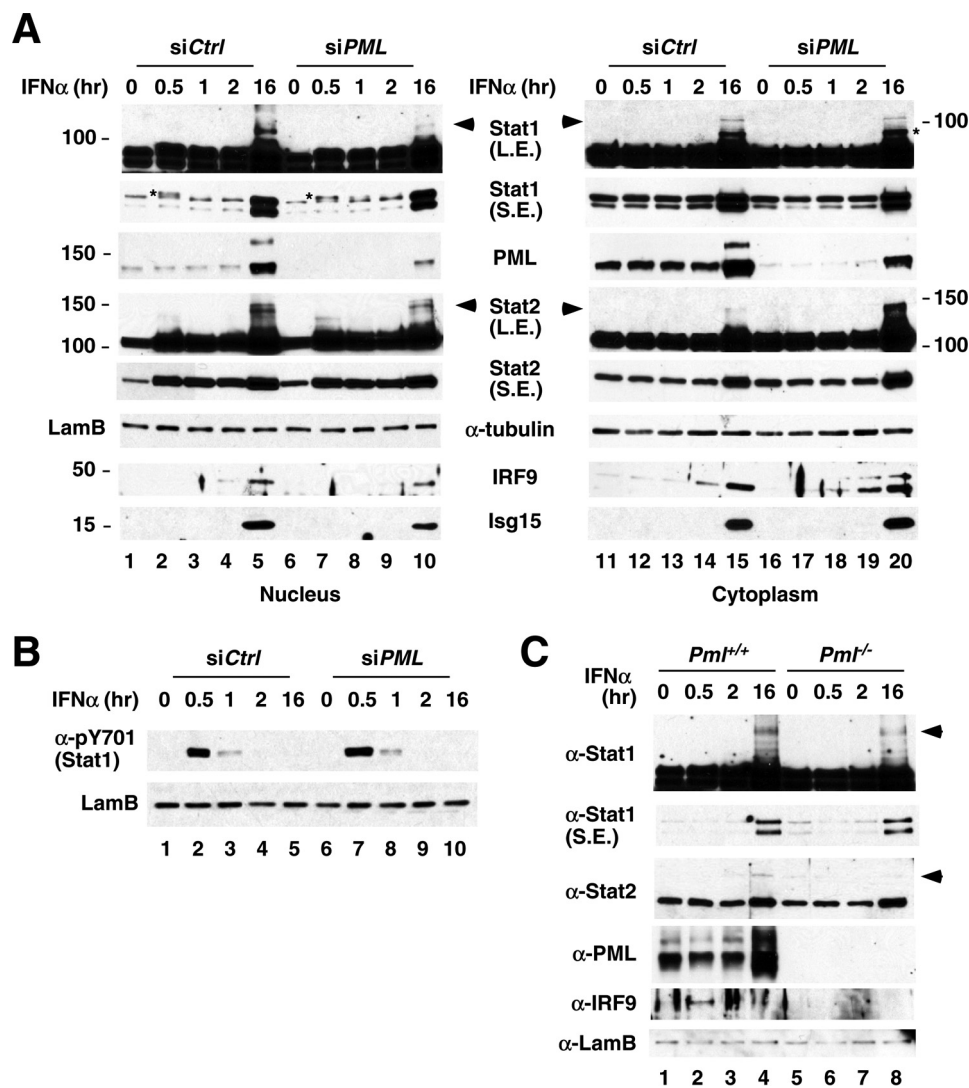
Figure 6. PML promoted Stat1 and Stat2 isgylation and affected ISGF3 complexes. *A*, HUVECs were transiently transfected with a control (si*Ctrl*) or a *PML* siRNA (si*PML*). 72 h later cells were treated with IFNα, harvested at 0, 0.5, 1, 2, and 16 h, and subcellular fractions were prepared. Nuclear (*lanes 1–10*) and cytoplasmic (*lanes 11–20*) fractions were subjected to Western blotting with the indicated antibodies. *L.E.*, long exposure; *S.E.*, short exposure. The *arrows* indicate Isg15-nStat1 and Isg15-nStat2. The *asterisk* marks an unknown Stat1 species, likely to be Tyr(P)-701-Stat1. Lamin B and α-tubulin were used as markers for nuclear and cytoplasmic fractions, respectively. *B*, the effect of *PML* KD on the abundance of Tyr(P)-701-Stat1. Nuclear fractions from *A* were subjected to Western blotting with anti-Tyr(P)-701-Stat1 antibody. *C*, aortic ECs from *Pml*⁻/⁻ show decreased Isg15-nStat1, Isg15-nStat2, and nIRF9. Aortic ECs isolated from aortic rings of WT and *Pml*⁻/⁻ mice were treated with IFNα (10³ units/ml) and harvested at the indicated times, and subcellular fractions were prepared. The nuclear fractions were subjected to Western blotting with the indicated antibodies.

hypothesis, we carried out wound healing and *in vitro* capillary tube formation and determined whether LLL12, a selective Stat3 small molecule inhibitor, has effects on EC migration and tube formation in *PML* KD ECs. Our data indicated that LLL12 inhibited increased EC migration and capillary tube formation in *PML* KD HUVECs upon IFNα stimulation (Fig. 8, *F* and *G*).

Discussion

Upon IFNα stimulation, both Stat1 and Stat3 are phosphorylated and translocated into the nucleus binding to specific DNA regions to control gene expression. However, the activated Stat3 in the nucleus is transient and only found during the early phase of IFN stimulation (19, 43). The simultaneously activated opposing activities of Stat1 (angiostatic) and Stat3 (angiogenic) ensure forced amplification (feedforward) or timely attenuation (feedback) of the biological effects of a given

dose of IFNα. PML has been known as an interferon-stimulated gene with the potential to block angiogenesis (6, 44). Thus, a link between IFNα, PML, and anti-angiogenesis is intriguing. Our results demonstrate that PML has a dual activity in positively regulating Stat1 activity and negatively regulating Stat3 activity through isgylation and protein stability control, respectively. Thus, as one of the ISGs, PML has a unique role in controlling Stat1 and Stat3 activity, thereby contributing to IFNα-mediated inhibition of angiogenesis. Our findings further support a concept that under certain circumstances, such as *PML* deficiency, IFNα may reduce or even lose its anti-angiogenic activity due to alteration of the balance between Stat1 and Stat3, [Stat1]/[Stat3] (Fig. 1). Several anti-cancer or anti-inflammation drugs are direct or indirect PML inducers or suppressors and require PML for their therapeutic activity (45, 46). As such, our data raise the possibility for anti-angiogenic ther-
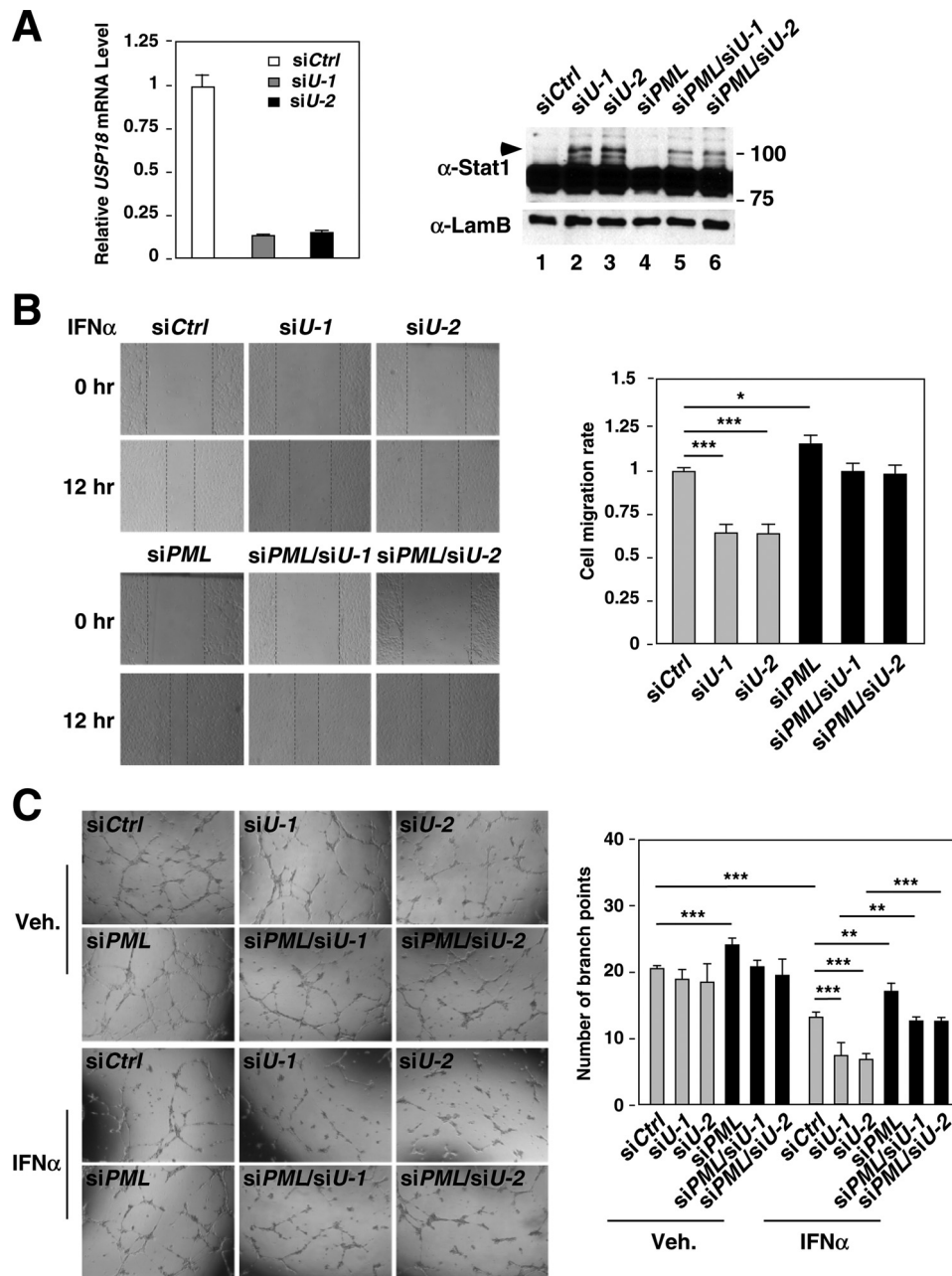
Figure 7. The effect of *USP18* knockdown on IFNα-mediated Stat1 isgylation, EC migration, and capillary tube formation. *A*, HUVECs were transiently transfected with a control (si*Ctrl*), *USP18* (si*U*), or *PML* (si*PML*) siRNAs for 48 h and trypsinized, and equal amounts of cells were seeded in 6-well plates. The levels of Stat1 and Stat1 isgylation were detected by Western blotting using antibodies against Stat1. Lamin B was used as a loading control. *Arrows*: isgylated Stat1. *B*, the *left panel* shows representative results of wound healing assays. The cell migration rates were quantified and are shown on the *right panel*. The statistical results are the mean ± S.D. ($n = 6$) (*, $p < 0.05$; ***, $p < 0.001$; unpaired two-tailed t test). *C*, *PML* and *USP18* in HUVECs were knocked down by the indicated siRNAs. Cells were then treated with IFNα (10^3 units/ml) for 16 h followed by capillary tube formation assays. Representative images are shown on the *left*. The numbers of braches in each field were counted, and the quantitative results are shown in the *right panel*. The statistical results are mean ± S.D. ($n = 6$) (**, $p < 0.01$; ***, $p < 0.001$; unpaired two-tailed t test).

apies in which patients are simultaneously treated with IFNα- and PML-altering agents.

There are several reports demonstrating that Stat1 transcriptionally activates *PML* expression (6, 47, 48). Our study is the first reporting that PML directly regulates Stat1 activity, indicating that there is a PML-Stat1 axis that forms a positive feedforward loop to mediate IFNα-induced angiostatic activity (6). A large cohort of ISGs is regulated by both PML and the unphosphorylated active form of Stat1, supporting a role for PML and Stat1 in the same IFN regulatory axis (Fig. 2, *B* and *C*). It is

known that Stat1 transcriptionally activates its own promoter (49). Thus, the decrease in *STAT1* mRNA and Stat1 target gene expression is a consequence of reduced Stat1 activity in *PML* KD cells. Among these PML target genes, Stat1 has been demonstrated as a negative regulator of angiogenesis and Mx1, a GTPase known to inhibit cell migration and senescence (50, 51). Furthermore, we also observed decreased expression of several senescence secretory cytokines, such as *IL-1*, *CXCL1*, and *CXCL11*, in *PML* KD HUVECs. Taken together, our findings support the concept that PML mediates IFN-induced EC
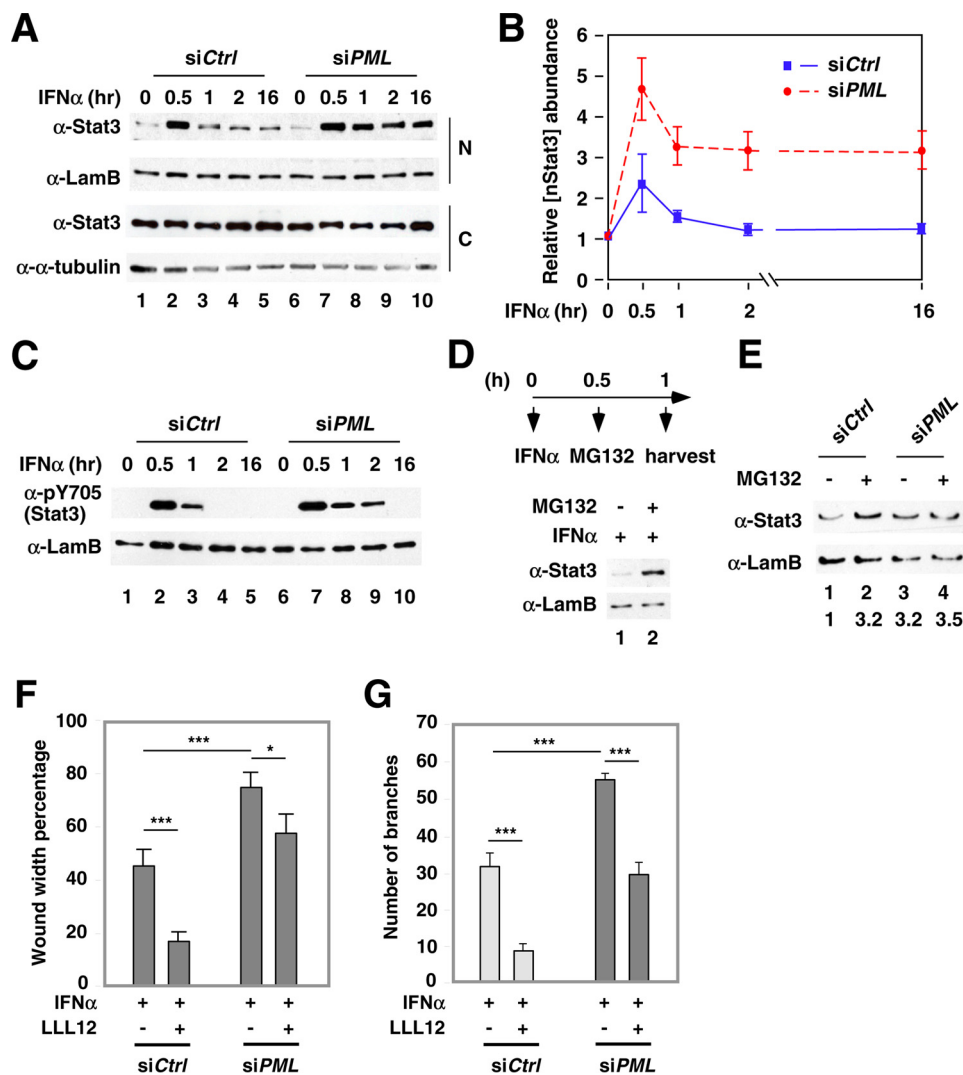
Figure 8. PML negatively regulated nStat3 stability and attenuated Stat3 function in EC network formation. *A*, accumulation of Tyr(P)-705-nStat3 in *PML* KD HUVECs. Procedures were the same as that described in Fig. 6, except that Stat3 and Tyr(P)-705-Stat3 antibodies were used for Western blotting. *B*, quantification of nStat3 protein abundance from *A*. The relative abundance of Stat3 at each time point was normalized to that at 0 h of IFNα treatment (*lanes 1* and *6*). *n* = 5. *C*, samples from *A* were subjected to Western blotting with anti-Tyr(P)-705-Stat3 antibody. *D*, MG132 increased nStat3 after 0.5 h of IFNα treatment. HUVECs were treated with 0.5 h of IFNα (10^3 units/ml) followed by 0.5 h of treatment with vehicle or MG132 and harvested, nuclear fractions were prepared and Western-blotted with the indicated antibodies. *E*, knockdown of PML abolished MG132-mediated accumulation of nStat3 in response to IFNα stimulation. *F*, control and *PML* KD HUVECs were pretreated with LLL12 (100 nM) for 3 h and trypsinized. Equal numbers of cells were subjected to wound-healing assays and capillary tube formation assays in the presence of IFNα (*G*). Statistical analysis was performed by counting numbers of branch points per field at 6 and 21 h of the assay. *n* = 6 per group (*, $p < 0.05$; ***, $p < 0.001$; unpaired two-tailed *t* test).

senescence and inhibition of angiogenesis (52, 53), in part, by potentiating Stat1 activity.

Mechanistically, PML mediates IFNα activity by promoting isgylation of Stat1 and Stat2 (Figs. 3–6). This is evident by the experiments with knockdown of *ISG15* or *USP18* and further validated in primary ECs isolated from WT and *Pml* KO mice (Fig. 6). Although Stat1 isgylation has been reported previously (21), we are the first to demonstrate that Stat2 is isgylated. It was proposed that the isgylation potentiates ISGF3 function and augments IFNα signaling to promote cellular senescence and anti-viral activity (39, 40). Notably, our data demonstrated that protein isgylation promotes the inhibitory effect of the IFN-PML axis on EC migration and network formation (Fig. 7). However, the detailed mechanism by which isgylation enhances Stat1/Stat2 activity remains unknown, whereas it has been proposed that isgylation may regulate protein synthesis or protein stability (24, 25, 54). Mapping the isgylated residues in Stat1 and Stat2 and validating the defect of Stat1/2 isgylation incompetent mutants will help address this issue in the future.

Stat3 is a well known oncogene and angiogenesis promoter (43, 55, 56). PML is known to directly interact with Stat3 and inhibit Stat3 activity by sequestering Stat3 in PML NBs (57, 58) or by interfering Stat3-HDAC3 interaction (59). Interestingly, we found that PML negatively regulates nuclear Stat3 abundance in response to IFNα treatment, partially by increasing proteasome-mediated Stat3 turnover (Fig. 8, *A–E*). Although several studies have suggested partial co-localization between components of proteasomes and PML NBs (60, 61) and a potential role of PML NBs in promoting protein degradation (62), the detailed mechanism by which PML promotes Stat3 turnover awaits future investigation. Furthermore, our data indicate that PML and Stat3 share a set of common target genes

(supplemental Tables 1 and 2). Of those genes, *DCBLD2*, *ELF2*, and *CXCL11* are key angiogenic effectors and may contribute to PML-Stat3 axis-mediated angiogenesis regulation (63–66). Consistent with this PML-Stat3 negative feedback loop, loss of *PML* compromises that ability of LLL112, a Stat3 inhibitor, to inhibit EC migration and tube formation (Fig. 8, *F* and *G*).

Stat1 and Stat3 can form either homodimers or heterodimers, and the type and stoichiometry of Stat1-Stat3 complex formation may affect its DNA binding and alter the IFN-induced gene expression pattern (67). Several studies suggest that Stat3 is a negative regulator of Stat1 and that depletion of Stat3 increases IFN-mediated anti-viral activity (43, 68). Interestingly, a recent study demonstrated that knock-out of *Stat1* in murine macrophage sustained type I IFN-induced Stat3 phosphorylation (69), an observation similar to what we observed in *PML* KD HUVECs (Fig. 8, *A--E*). As such, the prolonged pStat3 in *Stat1* knock-out cells is presumably the outcome of the disturbed Stat1-PML-Stat3 regulatory network.

Our study uncovers PML as a key IFNα-signaling regulator that amplifies a positive feedforward loop with ISGF3 complex through isgylation system and counteracts IFN signaling suppressor Stat3 by controlling Stat3 abundance. Through this intricate regulation, PML augments the IFNα-Stat1 signaling in ECs and thus inhibits angiogenesis. Once PML function is lost, the overall IFNα activity tips toward enhancing Stat3 activity and, thus, enhances angiogenesis. Although our current study mainly focused IFNα-PML-Stats axis function on EC regulation, the outcome of reduced *in vivo* angiogenesis inhibition in *Pml* knock-out mouse may partially result from other microenvironmental factors and awaits further investigation. In conclusion, our observations suggested that elevation of PML protein levels in endothelium would promote IFNα anti-angiogenic activity and therapeutic effects.

Experimental procedures

Cell lines, reagents, and antibodies

HUVECs were purchased from Lonza and cultured in endothelial cell basal medium (EBM-2; Lonza) with EGM-2 SingleQuot growth supplements (Lonza). Cells that were <6 passages were used in this study. LLL12 was purchased from EMD Millipore. MG132 was purchased from Sigma, recombinant human IFNα was purchased from R&D system, and recombinant mouse IFNα was purchased from PBL assay science. siRNAs were purchased from Thermo Scientific and are listed in the supplemental Table 4. Antibodies used in this study are listed in supplemental Table 3 and are tested in supplemental Figure 1. The transfection reagent DharmaFECT1 (T-2001) was purchased from Thermo Scientific.

siRNA knockdown and subcellular fractionation

A non-targeting siRNA or independent siRNAs against *USP18*, *PML*, *or ISG15* were transfected into HUVECs using DF1 transfection reagent (Thermo Scientific) according to previous protocol (70). Cells were harvested at 72 h after siRNA transfection before preparation of total RNA or nuclear and cytoplasmic fractionation. Before harvest cells were treated with MG132 (50 μg/ml) or IFNα (10^3 units/ml) for the indicated times. For nuclear and cytoplasmic fractionation,

HUVECs were washed with 1× PBS one time and spun down using a desktop centrifuge at 4 °C, 5000 rpm for 5 min. The cell pellets were resuspended in 5× the pellet volume in cytosolic fractionation buffer (10 mM Tris, pH 7.4, 10 mM NaCl, 3 mM $MgCl_2$, 0.5%Nonidet P-40, and 5% glycerol) and kept on ice for 10 min. The nuclei were collected by centrifugation at 4000 rpm for 6 min, and the supernatants (1st cytosolic fraction) were transferred to a new tube. The pellets were resuspended in cytosolic fractionation buffer and spun down again. The supernatant was collected and combined with the 1st extract as the cytosolic fraction. The resulting nuclear pellets were resuspended in nuclear fraction buffer (10 mM HEPES, pH 7.5, 400 mM NaCl, 5 mM EDTA, 0.5% Nonidet P-40, 1 mM DTT, and 5% glycerol) on ice for 15 min and vortexed every 5 min until completely homogenized. The prepared lysates were mixed with an equal volume of 2× SDS buffer (100 mM Tris-Cl, pH 6.8, 4% SDS, 0.2% bromphenol blue, 20% glycerol, and 2% β-mercaptoethanol) and boiled for 10 min. For Western blots, antibodies against Lamin B or α-tubulin served as the internal loading and recovery controls for nuclear and cytoplasmic fractions, respectively.

Total RNA extraction, RT-PCR, and qRT-PCR

HUVECs and mice aortic endothelial cells were harvested, and total RNA was prepared using PrepEase RNA Spin kits (U. S. Biochemical Corp./Affymetrix). Single-strand cDNA pools were generated using transcriptor universal cDNA master (Roche Applied Science) according to the manufacturer's instructions. The cDNAs of the target genes were quantified by qPCR using an iCycler (Bio-Rad) platform with 2×iQ SYBR Green Supermix (Bio-Rad) and appropriate primer sets as listed in supplemental Table 3. The PCR program was set for 40 cycles with three steps of 95 °C for 30 s, 55 °C for 30 s, and 72 °C for 30 s. Melting curves were obtained after each cycle to ensure the homogeneity of the PCR products. The relative abundance of target genes was normalized to an internal control (18S rRNA) and are depicted as the mean ± S.D. from three independent experiments.

Examination of IFNα-induced Stat1/Stat2 isgylation

The si*Control*, si*Usp18*, and si*ISG15* HUVECs were treated with INFα (10^3 units/ml) for 16 h. After collection, the nuclear fractions were prepared with a mixture of protease inhibitors (Roche Applied Science). The lysates were precleaned with protein A beads and immunoprecipitated with anti-Stat1, Stat2, or Isg15 antibodies. The immunoprecipitates were pulled down by protein A beads and subjected to Western blotting with the indicated antibodies.

Capillary tube formation assay

HUVECs were transiently transfected with the indicated siRNAs. Cells were treated with trypsin, and 10^4 cells were plated on Matrigel (Millipore) in 96-well plates. After seeding on the gel for 2 h, cells were treated with or without INFα (10^3 units/ml) in the culture medium for 12 h before image capture. Six fields per experimental group were randomly picked, and the branch points in each field were counted for statistical analysis. All results are shown as the mean ± S.D.

Wound healing assay

HUVECs were transiently transfected with siRNAs. The next day the cells were plated on 6-well dishes. Cells were grown to confluence and treated with IFNα (10^3 units/ml) for 4 h and followed by scratching with a sterile pipette tip to generate wounds with continued IFNα treatment. At 0 and 12 h after scratching, images of 6 randomly chosen fields were captured through a microscope equipped with a camera, and the width of the same wounds was measured by ImageJ. A portion of the treated cells was used for Western blotting. The cell migration rate was quantified by measuring the distance of the wound closure between 0 and 12 h. The results are shown as the mean ± S.D.

Isolation of mouse aortic endothelial cells

Both $Pml^{+/+}$ (WT) and $Pml^{-/-}$ (KO) mice were maintained in the $129^{S1/SvImJ}$ background with normal rodent chow and sterile water in the Health Science Animal Facility at Case Western Reserve University. All procedures were approved by the Case Western Reserve University Institutional Animal Care and Use Committees. The genotype of the mouse was confirmed by PCR analysis from tail biopsies. The mouse aortas were isolated, and periadventitial fat was removed. The sliced aortic rings were embedded into Matrigel (BD Biosciences) in EGM2 medium (Lonza) with 10% FBS (Sigma). After 3 days the gel-embedded aortic rings were collected and treated with trypsin. Endothelial cells were resuspended in EGM2 medium with 5% FBS and cultured on the fibronectin-coated culture dishes. The endothelial cells used in the study were from passages 2–3.

In vivo Matrigel plug assay

In vivo Matrigel plug assays were performed according to our published protocol (38). To implant plugs, wild-type and *Pml* KO mice at 8 weeks of age were subcutaneously injected with 1 ml/mouse of Matrigel on an abdominal site adjacent to, but not overlapping abdominal blood vessels. The base Matrigel contained a mixture of Matrigel (BD Biosciences) with 60 ng/ml VEGF-A and 60 units/ml heparin. The vehicle control was 0.1% BSA in 1×PBS. For cytokine treatment, mouse TNFα or IFNα was added to a final concentration of 50 ng/ml. Two weeks after injection, the mice were euthanized, and the Matrigel plugs were isolated. For quantification purposes, ~200 mg plugs were homogenized in Drabkin's solution (Sigma, D5941), and optical density was measured at 540 nm and then normalized to the weight of the plugs.

Statistical analysis

Data are presented as the mean ± S.D. of three independent experiments. Two compared groups were analyzed by two-tailed Student's *t* test. Statistical significance is presented as: *n.s.*, not significance; *, $p < 0.05$; **, $p < 0.01$; ***, $p < 0.001$.

References

1. Gutterman, J. U. (1994) Cytokine therapeutics: lessons from interferon α. *Proc. Natl. Acad. Sci. U.S.A.* **91,** 1198–1205
2. Borden, E. C., Sen, G. C., Uze, G., Silverman, R. H., Ransohoff, R. M., Foster, G. R., and Stark, G. R. (2007) Interferons at age 50: past, current, and future impact on biomedicine. *Nat. Rev. Drug Discov.* **6,** 975–990
3. Liu, F., Gao, X., Wang, J., Gao, C., Li, X., Li, X., Gong, X., and Zeng, X. (2016) Transcriptome sequencing to identify transcription factor regulatory network and alternative splicing in endothelial cells under VEGF stimulation. *J. Mol. Neurosci.* **58,** 170–177
4. Sgonc, R., Fuerhapter, C., Boeck, G., Swerlick, R., Fritsch, P., and Sepp, N. (1998) Induction of apoptosis in human dermal microvascular endothelial cells and infantile hemangiomas by interferon-α. *Int. Arch. Allergy Immunol.* **117,** 209–214
5. Albini, A., Marchisone, C., Del Grosso, F., Benelli, R., Masiello, L., Tacchetti, C., Bono, M., Ferrantini, M., Rozera, C., Truini, M., Belardelli, F., Santi, L., and Noonan, D. M. (2000) Inhibition of angiogenesis and vascular tumor growth by interferon-producing cells: a gene therapy approach. *Am. J. Pathol.* **156,** 1381–1393
6. Cheng, X., Liu, Y., Chu, H., and Kao, H. Y. (2012) Promyelocytic leukemia protein (PML) regulates endothelial cell network formation and migration in response to tumor necrosis factor α (TNFα) and interferon α (IFNα). *J. Biol. Chem.* **287,** 23356–23367
7. Dvorak, H. F., and Gresser, I. (1989) Microvascular injury in pathogenesis of interferon-induced necrosis of subcutaneous tumors in mice. *J. Natl. Cancer Inst.* **81,** 497–502
8. Miller, J. W., Stinson, W. G., and Folkman, J. (1993) Regression of experimental iris neovascularization with systemic α-interferon. *Ophthalmology* **100,** 9–14
9. Sidky, Y. A., and Borden, E. C. (1987) Inhibition of angiogenesis by interferons: effects on tumor- and lymphocyte-induced vascular responses. *Cancer Res.* **47,** 5155–5161
10. Levy, D. E., and Darnell, J. E., Jr. (2002) Stats: transcriptional control and biological impact. *Nat. Rev. Mol. Cell Biol.* **3,** 651–662
11. Stark, G. R., and Darnell, J. E., Jr. (2012) The JAK-STAT pathway at twenty. *Immunity* **36,** 503–514
12. Fu, X. Y., Schindler, C., Improta, T., Aebersold, R., and Darnell, J. E., Jr. (1992) The proteins of ISGF-3, the interferon α-induced transcriptional activator, define a gene family involved in signal transduction. *Proc. Natl. Acad. Sci. U.S.A.* **89,** 7840–7843
13. Schindler, C., Fu, X. Y., Improta, T., Aebersold, R., and Darnell, J. E., Jr. (1992) Proteins of transcription factor ISGF-3: one gene encodes the 91- and 84-kDa ISGF-3 proteins that are activated by interferon α. *Proc. Natl. Acad. Sci. U.S.A.* **89,** 7836–7839
14. Gomez, D., and Reich, N. C. (2003) Stimulation of primary human endothelial cell proliferation by IFN. *J. Immunol.* **170,** 5373–5381
15. Qing, Y., and Stark, G. R. (2004) Alternative activation of STAT1 and STAT3 in response to interferon-γ. *J. Biol. Chem.* **279,** 41679–41685
16. Ramana, C. V., Gil, M. P., Schreiber, R. D., and Stark, G. R. (2002) Stat1-dependent and -independent pathways in IFN-γ-dependent signaling. *Trends Immunol.* **23,** 96–101
17. Regis, G., Pensa, S., Boselli, D., Novelli, F., and Poli, V. (2008) Ups and downs: the STAT1:STAT3 seesaw of Interferon and gp130 receptor signalling. *Semin. Cell Dev. Biol.* **19,** 351–359
18. Cheon, H., Yang, J., and Stark, G. R. (2011) The functions of signal transducers and activators of transcriptions 1 and 3 as cytokine-inducible proteins. *J. Interferon Cytokine Res.* **31,** 33–40
19. Icardi, L., Lievens, S., Mori, R., Piessevaux, J., De Cauwer, L., De Bosscher, K., and Tavernier, J. (2012) Opposed regulation of type I IFN-induced STAT3 and ISGF3 transcriptional activities by histone deacetylases (HDACS) 1 and 2. *FASEB J.* **26,** 240–249
20. Zhang, D., and Zhang, D. E. (2011) Interferon-stimulated gene 15 and the protein ISGylation system. *J. Interferon Cytokine Res.* **31,** 119–130

≋ASBMB

21. Malakhov, M. P., Kim, K. I., Malakhova, O. A., Jacobs, B. S., Borden, E. C., and Zhang, D. E. (2003) High-throughput immunoblotting: ubiquitin-like protein ISG15 modifies key regulators of signal transduction. *J. Biol. Chem.* **278,** 16608–16613

22. Ungureanu, D., Vanhatupa, S., Kotaja, N., Yang, J., Aittomaki, S., Jänne, O. A., Palvimo, J. J., and Silvennoinen, O. (2003) PIAS proteins promote SUMO-1 conjugation to STAT1. *Blood* **102,** 3311–3313

23. Sgorbissa, A., and Brancolini, C. (2012) IFNs, ISGylation and cancer: cui prodest? *Cytokine Growth Factor Rev.* **23,** 307–314

24. Huang, Y. F., Wee, S., Gunaratne, J., Lane, D. P., and Bulavin, D. V. (2014) Isg15 controls p53 stability and functions. *Cell Cycle* **13,** 2200–2210

25. Fan, J.-B., Arimoto, K-l., Motamedchaboki, K., Yan, M., Wolf, D. A., and Zhang, D.-E. (2015) Identification and characterization of a novel ISG15-ubiquitin mixed chain and its role in regulating protein homeostasis. *Sci. Rep.* **5,** 12704

26. Malakhova, O. A., Yan, M., Malakhov, M. P., Yuan, Y., Ritchie, K. J., Kim, K. I., Peterson, L. F., Shuai, K., and Zhang, D. E. (2003) Protein ISGylation modulates the JAK-STAT signaling pathway. *Genes Dev.* **17,** 455–460

27. Richer, E., Prendergast, C., Zhang, D. E., Qureshi, S. T., Vidal, S. M., and Malo, D. (2010) *N*-Ethyl-*N*-nitrosourea-induced mutation in ubiquitin-specific peptidase 18 causes hyperactivation of IFN-αß signaling and suppresses STAT4-induced IFN-γ production, resulting in increased susceptibility to *Salmonella typhimurium. J. Immunol.* **185,** 3593–3601

28. Dyck, J. A., Maul, G. G., Miller, W. H., Jr, Chen, J. D., Kakizuka, A., and Evans, R. M. (1994) A novel macromolecular structure is a target of the promyelocyte-retinoic acid receptor oncoprotein. *Cell* **76,** 333–343

29. de Thé, H., Lavau, C., Marchio, A., Chomienne, C., Degos, L., and Dejean, A. (1991) The PML-RAR α fusion mRNA generated by the t(15;17) translocation in acute promyelocytic leukemia encodes a functionally altered RAR. *Cell* **66,** 675–684

30. Kakizuka, A., Miller, W. H., Jr, Umesono, K., Warrell, R. P., Jr, Frankel, S. R., Murty, V. V., Dmitrovsky, E., and Evans, R. M. (1991) Chromosomal translocation t(15;17) in human acute promyelocytic leukemia fuses RAR α with a novel putative transcription factor, PML. *Cell* **66,** 663–674

31. Bernardi, R., Papa, A., and Pandolfi, P. P. (2008) Regulation of apoptosis by PML and the PML-NBs. *Oncogene* **27,** 6299–6312

32. Gurrieri, C., Capodieci, P., Bernardi, R., Scaglioni, P. P., Nafa, K., Rush, L. J., Verbel, D. A., Cordon-Cardo, C., and Pandolfi, P. P. (2004) Loss of the tumor suppressor PML in human cancers of multiple histologic origins. *J. Natl. Cancer Inst.* **96,** 269–279

33. Hsu, K. S., Guan, B. J., Cheng, X., Guan, D., Lam, M., Hatzoglou, M., and Kao, H. Y. (2016) Translational control of PML contributes to TNFα-induced apoptosis of MCF7 breast cancer cells and decreased angiogenesis in HUVECs. *Cell Death Differ.* **23,** 469–483

34. Yamada, N., Tsujimura, N., Kumazaki, M., Shinohara, H., Taniguchi, K., Nakagawa, Y., Naoe, T., and Akao, Y. (2014) Colorectal cancer cell-derived microvesicles containing microRNA-1246 promote angiogenesis by activating Smad 1/5/8 signaling elicited by PML down-regulation in endothelial cells. *Biochim. Biophys. Acta* **1839,** 1256–1272

35. Cheng, X., and Kao, H. Y. (2012) Microarray analysis revealing common and distinct functions of promyelocytic leukemia protein (PML) and tumor necrosis factor α (TNFα) signaling in endothelial cells. *BMC Genomics* **13,** 453

36. Indraccolo, S., Pfeffer, U., Minuzzo, S., Esposito, G., Roni, V., Mandruzzato, S., Ferrari, N., Anfosso, L., Dell'Eva, R., Noonan, D. M., Chieco-Bianchi, L., Albini, A., and Amadori, A. (2007) Identification of genes selectively regulated by IFNs in endothelial cells. *J. Immunol.* **178,** 1122–1135

37. Cheon, H., and Stark, G. R. (2009) Unphosphorylated STAT1 prolongs the expression of interferon-induced immune regulatory genes. *Proc. Natl. Acad. Sci. U.S.A.* **106,** 9373–9378

38. Mahabeleshwar, G. H., Chen, J., Feng, W., Somanath, P. R., Razorenova, O. V., and Byzova, T. V. (2008) Integrin affinity modulation in angiogenesis. *Cell Cycle* **7,** 335–347

39. Randall, G., Chen, L., Panis, M., Fischer, A. K., Lindenbach, B. D., Sun, J., Heathcote, J., Rice, C. M., Edwards, A. M., and McGilvray, I. D. (2006) Silencing of USP18 potentiates the antiviral activity of interferon against hepatitis C virus infection. *Gastroenterology* **131,** 1584–1591

40. Santin, I., Moore, F., Grieco, F. A., Marchetti, P., Brancolini, C., and Eizirik, D. L. (2012) USP18 is a key regulator of the interferon-driven gene network modulating pancreatic beta cell inflammation and apoptosis. *Cell Death Dis.* **3,** e419

41. Dauer, D. J., Ferraro, B., Song, L., Yu, B., Mora, L., Buettner, R., Enkemann, S., Jove, R., and Haura, E. B. (2005) Stat3 regulates genes common to both wound healing and cancer. *Oncogene* **24,** 3397–3408

42. Hurley, D., Araki, H., Tamada, Y., Dunmore, B., Sanders, D., Humphreys, S., Affara, M., Imoto, S., Yasuda, K., Tomiyasu, Y., Tashiro, K., Savoie, C., Cho, V., Smith, S., Kuhara, S., *et al.* (2012) Gene network inference and visualization tools for biologists: application to new human transcriptome datasets. *Nucleic Acids Res.* **40,** 2377–2398

43. Avalle, L., Pensa, S., Regis, G., Novelli, F., and Poli, V. (2012) STAT1 and STAT3 in tumorigenesis. *JAK-STAT* **1,** 65–72

44. Grötzinger, T., Sternsdorf, T., Jensen, K., and Will, H. (1996) Interferon-modulated expression of genes encoding the nuclear-dot-associated proteins Sp100 and promyelocytic leukemia protein (PML). *Eur. J. Biochem.* **238,** 554–560

45. Wolyniec, K., Carney, D. A., Haupt, S., and Haupt, Y. (2013) New strategies to direct therapeutic targeting of PML to treat cancers. *Front. Oncol.* **3,** 124

46. Sahin, U., Lallemand-Breitenbach, V., and de Thé, H. (2014) PML nuclear bodies: regulation, function, and therapeutic perspectives. *J. Pathol.* **234,** 289–291

47. Stadler, M., Chelbi-Alix, M. K., Koken, M. H., Venturini, L., Lee, C., Saïb, A., Quignon, F., Pelicano, L., Guillemin, M. C., and Schindler, C. (1995) Transcriptional induction of the PML growth suppressor gene by interferons is mediated through an ISRE and a GAS element. *Oncogene* **11,** 2565–2573

48. Chelbi-Alix, M. K., Pelicano, L., Quignon, F., Koken, M. H., Venturini, L., Stadler, M., Pavlovic, J., Degos, L., and de Thé, H. (1995) Induction of the PML protein by interferons in normal and APL cells. *Leukemia* **9,** 2027–2033

49. Yuasa, K., and Hijikata, T. (2016) Distal regulatory element of the STAT1 gene potentially mediates positive feedback control of STAT1 expression. *Genes Cells* **21,** 25–40

50. Mushinski, J. F., Nguyen, P., Stevens, L. M., Khanna, C., Lee, S., Chung, E. J., Lee, M. J., Kim, Y. S., Linehan, W. M., Horisberger, M. A., and Trepel, J. B. (2009) Inhibition of tumor cell motility by the interferon-inducible GTPase MxA. *J. Biol. Chem.* **284,** 15206–15214

51. Horisberger, M. A. (1992) Interferon-induced human protein MxA is a GTPase which binds transiently to cellular proteins. *J. Virol.* **66,** 4705–4709

52. Novakova, Z., Hubackova, S., Kosar, M., Janderova-Rossmeislova, L., Dobrovolna, J., Vasicova, P., Vancurova, M., Horejsi, Z., Hozak, P., Bartek, J., and Hodny, Z. (2010) Cytokine expression and signaling in drug-induced cellular senescence. *Oncogene* **29,** 273–284

53. Balestrieri, M. L., Balestrieri, A., Mancini, F. P., and Napoli, C. (2008) Understanding the immunoangiostatic CXC chemokine network. *Cardiovasc. Res.* **78,** 250–256

54. Durfee, L. A., Lyon, N., Seo, K., and Huibregtse, J. M. (2010) The ISG15 conjugation system broadly targets newly synthesized proteins: implications for the antiviral function of ISG15. *Mol. Cell* **38,** 722–732

55. Niu, G., Wright, K. L., Huang, M., Song, L., Haura, E., Turkson, J., Zhang, S., Wang, T., Sinibaldi, D., Coppola, D., Heller, R., Ellis, L. M., Karras, J., Bromberg, J., Pardoll, D., Jove, R., and Yu, H. (2002) Constitutive Stat3 activity up-regulates VEGF expression and tumor angiogenesis. *Oncogene* **21,** 2000–2008

56. Wei, D., Le, X., Zheng, L., Wang, L., Frey, J. A., Gao, A. C., Peng, Z., Huang, S., Xiong, H. Q., Abbruzzese, J. L., and Xie, K. (2003) Stat3 activation regulates the expression of vascular endothelial growth factor and human pancreatic cancer angiogenesis and metastasis. *Oncogene* **22,** 319–329

57. Kawasaki, A., Matsumura, I., Kataoka, Y., Takigawa, E., Nakajima, K., and Kanakura, Y. (2003) Opposing effects of PML and PML/RAR α on STAT3 activity. *Blood* **101,** 3668–3673

58. Ohbayashi, N., Kawakami, S., Muromoto, R., Togi, S., Ikeda, O., Kamitani, S., Sekine, Y., Honjoh, T., and Matsuda, T. (2008) The IL-6 family of

cytokines modulates STAT3 activation by desumoylation of PML through SENP1 induction. *Biochem. Biophys. Res. Commun.* **371,** 823– 828

59. Kato, M., Muromoto, R., Togi, S., Iwakami, M., Kitai, Y., Kon, S., Oritani, K., and Matsuda, T. (2015) PML suppresses IL-6-induced STAT3 activation by interfering with STAT3 and HDAC3 interaction. *Biochem. Biophys. Res. Commun.* **461,** 366 –371

60. Dino Rockel, T., and von Mikecz, A. (2002) Proteasome-dependent processing of nuclear proteins is correlated with their subnuclear localization. *J. Struct. Biol.* **140,** 189 –199

61. Fabunmi, R. P., Wigley, W. C., Thomas, P. J., and DeMartino, G. N. (2001) Interferon γ regulates accumulation of the proteasome activator PA28 and immunoproteasomes at nuclear PML bodies. *J. Cell Sci.* **114,** 29 –36

62. Guo, L., Giasson, B. I., Glavis-Bloom, A., Brewer, M. D., Shorter, J., Gitler, A. D., and Yang, X. (2014) A cellular system that degrades misfolded proteins and protects against neurodegeneration. *Mol. Cell* **55,** 15–30

63. Nie, L., Guo, X., Esmailzadeh, L., Zhang, J., Asadi, A., Collinge, M., Li, X., Kim, J. D., Woolls, M., Jin, S. W., Dubrac, A., Eichmann, A., Simons, M., Bender, J. R., and Sadeghi, M. M. (2013) Transmembrane protein ESDN promotes endothelial VEGF signaling and regulates angiogenesis. *J. Clin. Invest.* **123,** 5082–5097

64. Romagnani, P., Annunziato, F., Lasagni, L., Lazzeri, E., Beltrame, C., Francalanci, M., Uguccioni, M., Galli, G., Cosmi, L., Maurenzig, L., Baggiolini, M., Maggi, E., Romagnani, S., and Serio, M. (2001) Cell cycle-dependent expression of CXC chemokine receptor 3 by endothelial cells mediates angiostatic activity. *J. Clin. Invest.* **107,** 53– 63

65. Hamik, A., Wang, B., and Jain, M. K. (2006) Transcriptional regulators of angiogenesis. *Arterioscler. Thromb. Vasc. Biol.* **26,** 1936 –1947

66. Dube, A., Akbarali, Y., Sato, T. N., Libermann, T. A., and Oettgen, P. (1999) Role of the Ets transcription factors in the regulation of the vascular-specific Tie2 gene. *Circ. Res.* **84,** 1177–1185

67. Ho, H. H., and Ivashkiv, L. B. (2006) Role of STAT3 in type I interferon responses: negative regulation of STAT1-dependent inflammatory gene activation. *J. Biol. Chem.* **281,** 14111–14118

68. Wang, W. B., Levy, D. E., and Lee, C. K. (2011) STAT3 negatively regulates type I IFN-mediated antiviral response. *J. Immunol.* **187,** 2578 –2585

69. Kim, H. S., Kim, D. C., Kim, H.-M., Kwon, H.-J., Kwon, S. J., Kang, S.-J., Kim, S. C., and Choi, G.-E. (2015) STAT1 deficiency redirects IFN signalling toward suppression of TLR response through a feedback activation of STAT3. *Sci. Rep.* **5,** 13414

70. Ryo, A., Suizu, F., Yoshida, Y., Perrem, K., Liou, Y.-C., Wulf, G., Rottapel, R., Yamaoka, S., and Lu, K. P. (2003) Regulation of NF-κB Signaling by Pin1-dependent prolyl isomerization and ubiquitin-mediated proteolysis of p65/RelA. *Mol. Cell* **12,** 1413–1426